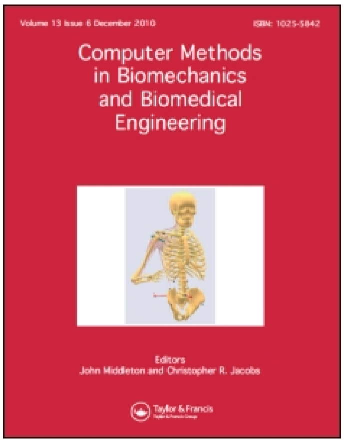

Computer Methods in Biomechanics and Biomedical Engineering
Publication details, including instructions for authors and subscription information:
http://www.informaworld.com/smpp/title~content=t713455284

Consistent formulation of the growth process at the kinematic and constitutive level for soft tissues composed of multiple constituents

H. Schmid[a]; L. Pauli[a]; A. Paulus[a]; E. Kuhl[b]; M. Itskov[a]
[a] Department of Continuum Mechanics, RWTH Aachen University, Aachen, Germany [b] Department of Mechanical Engineering, Stanford University, Stanford, CA, USA

First published on: 23 February 2011

Computer Methods in Biomechanics and Biomedical Engineering
iFirst article, 2011, 1–15

Taylor & Francis
Taylor & Francis Group

Consistent formulation of the growth process at the kinematic and constitutive level for soft tissues composed of multiple constituents

H. Schmid[a]*, L. Pauli[a], A. Paulus[a], E. Kuhl[b] and M. Itskov[a]

[a]*Department of Continuum Mechanics, RWTH Aachen University, Eilfschornsteinstrasse 18, 56062 Aachen, Germany;* [b]*Department of Mechanical Engineering, Stanford University, 496 Lomita Mall, Durand 217, Stanford, CA, USA*

(*Received 1 July 2010; final version received 13 December 2010*)

Previous studies have investigated the possibilities of modelling the change in volume and change in density of biomaterials. This can be modelled at the constitutive or the kinematic level. This work introduces a consistent formulation at the kinematic and constitutive level for growth processes. Most biomaterials consist of many constituents and can be approximated as being incompressible. These two conditions (many constituents and incompressibility) suggest a straightforward implementation in the context of the finite element (FE) method which could now be validated more easily against histological measurements. Its key characteristic variable is the normalised partial mass change. Using the concept of homeostatic equilibrium, we suggest two complementary growth laws in which the evolution of the normalised partial mass change is governed by an ordinary differential equation in terms of either the Piola–Kirchhoff stress or the Green–Lagrange strain. We combine this approach with the classical incompatibility condition and illustrate its algorithmic implementation within a fully nonlinear FE approach. This approach is first illustrated for a simple uniaxial tension and extension test for pure volume change and pure density change and is validated against previous numerical results. Finally, a physiologically based example of a two-phase model is presented which is a combination of volume and density changes. It can be concluded that the effect of hyper-restoration may be due to the systemic effect of degradation and adaptation of given constituents.

Keywords: volume growth; density change; incompressibility; growth and remodelling; adaptation; homeostatic equilibrium

Nomenclature

$\mathbf{F}^\tau(t)$	deformation gradient tensor at time (τ, t)
$\mathbf{F}_e^\tau(t)$	elastic part of the deformation gradient tensor at time (τ, t)
$\mathbf{F}_g^\tau(t)$	growth part of the deformation gradient tensor at time (τ, t)
J^τ	determinant of $\mathbf{F}^\tau(t)$
J_e^τ	determinant of $\mathbf{F}_e^\tau(t)$
J_g^τ	determinant of $\mathbf{F}_g^\tau(t)$
$\mathbf{C}^\tau(t)$	total right Cauchy–Green tensor at time (τ, t)
$\mathbf{C}_e^\tau(t)$	elastic right Cauchy–Green tensor at time (τ, t)
$\mathbf{E}^\tau(t)$	Green–Lagrange strain tensor at time (τ, t)
$\mathbf{P}^\tau(t)$	1st Piola–Kirchhoff stress tensor at time (τ, t)
$\mathbf{S}^\tau(t)$	2nd Piola–Kirchhoff stress tensor at time (τ, t)
$\boldsymbol{\sigma}^\tau(t)$	Cauchy stress tensor at time (τ, t)
$\Psi^\tau(t)$	free energy at time (τ, t)
$\mathbf{x}^\tau$	material point at time (τ, t)
$\mathbf{X}$	material point at time (0, 0)
θ_γ^τ	normalised density of constituent γ at time τ
ρ_γ^τ	density of constituent γ at time τ
r_γ^τ	partial density of constituent γ at time τ
ϕ_γ^τ	partial volume fraction of constituent γ at time τ
f_γ^τ	normalised partial mass change of constituent γ at time τ
ς_γ^τ	normalised partial density change of constituent γ at time τ
ν_γ^τ	normalised partial volume change of constituent γ at time τ
ν^τ	normalised tissue volume change at time τ
d	infinitesimal
d	differential
C	number of constituents
	Note that time t is being omitted in most cases, because it is clear from the context

1. Introduction

The objective of this contribution is the introduction of a novel formulation for growth and remodelling. Biological materials, in particular, commonly adapt their mass and their structure to environmental stimuli like stress or inflammation. For the modelling of biological materials with changing mass, two different approaches can be distinguished: the coupling of mass changes at the constitutive level and at the kinematic level. The given formulation is particularly attractive for incompressible tissues, because it utilises the fact that growth and remodelling are a large

*Corresponding author. Email: schmid@km.rwth-aachen.de

ISSN 1025-5842 print/ISSN 1476-8259 online

DOI: 10.1080/10255842.2010.548325
http://www.informaworld.com

timescale effects, whereas incompressibility can be considered as a short timescale phenomenon.

A change in mass can be characterised via a multiplicative decomposition of the deformation gradient tensor into a growth part and an elastic part. The decomposition was first introduced in the context of plasticity by Lee (1969). This approach is utilised for the kinematic coupling and was introduced by Rodriguez et al. (1994) to model soft biological tissues such as the arterial wall and the heart by assuming that the material response is described by one constitutive equation. Growth can be described as isotropically or more generally as transversely isotropic or orthotropically, see, e.g. Taber (1995), Menzel (2005, 2007), Himpel (2007) and Garikipati (2009). One of the prominent features is that the evolution equation for the internal variables (e.g. the isotropic growth stretch ratio (Himpel et al. 2005)) is derived on the basis of thermodynamic considerations. Most of these descriptions are able to represent volume growth by assuming a constant density; thus, mass change is realised by adding volume.

Mass change at the constitutive level, on the other hand, may be realised in a single-constituent setting by a weighting of the free energy function with respect to the density field as experimentally motivated (Cowin and Hegedus 1976; Carter and Hayes 1977). In this setting, the evolution equation for the internal variable (e.g. the mass source (Himpel et al. 2005)) is also thermodynamically consistent. These descriptions tend to describe density growth by assuming that volume stays constant, and thus the mass change happens by a change in density.

Most soft biological tissues, however, may be modelled as composites consisting of a number of constituents, either isotropic or anisotropic. Mixture theory is one of the possible approaches to model this. Humphrey and Rajagopal (2002) have been among the first to propose a constrained mixture theory formulation. In this description, they assumed that each constituent had a separate natural configuration. Klisch et al. (2003) used a similar formulation for describing cartilage tissue, although they referred each constituent back to one configuration, which makes the treatment easier. Furthermore, they used growth equations derived earlier (Klisch et al. 2001) from thermodynamic considerations. Other studies like Machyshyn et al. (2010) used a similar approach for arterial tissue. Biological tissues are thermodynamically open systems and it may be more useful to formulate growth and remodelling in a way (1) that the formulation is consistent on the kinematic and constitutive level and (2) that the evolution equations are still phenomenological, yet based on direct experimental observations. This is the focus of this work. This may be particularly useful because the appropriate choice and quantitative validation of the growth tensor may prove to be difficult, whereas histological measurements of individual mass fractions or volume fractions are feasible (Fisher and Llaurado 1966; Rizzo et al. 1989; Gleason and Humphrey 2004).

To characterise tissue anisotropy, the mathematical framework on the basis of generalised invariants is used. One of the first to introduce this concept was Spencer (1984) followed by Weiss et al. (1996) in the context of living tissues. It was established subsequently by Holzapfel et al. (2000). For example, the medial layer of the arterial wall may be considered as a composite of ground matrix, elastin, collagen and vascular smooth muscle cells (Watton et al. 2004; Itskov et al. 2006; Ehret and Itskov 2007; Schmid et al. 2010).

The property of incompressibility can be used in the context of growth and remodelling as will be briefly highlighted in the sequel and in more detail in Section 2. Incompressible materials can, on the one hand, be modelled as nearly incompressible by splitting the deformation gradient tensor into a volumetric part and an isochoric part and formulating the free energy as depending on those two parts, usually by introducing a sum of two free energies. The volumetric part is then chosen to be very stiff which results in a nearly incompressible behaviour (Peng and Chang 1997). On the other hand, the resulting hydrostatic pressure field may be, e.g., split off as an independent field in the finite element (FE) approach (so-called hybrid formulations) via the variational principle of Hu–Washizu. The incompressibility is then enforced on an element basis (e.g. Bathe 1982; Nash and Hunter 2000).

The timescale of the momentum balance is usually considered in the order of seconds. Yet, growth and remodelling take place in the order of days to weeks if not months. Thus, it has become a common practice to neglect the convective term in the continuity equation.[1] Although on the short timescale the material remains incompressible, the element volume, which is used in the FE context to enforce incompressibility, may then change as a consequence of a change in mass on the long timescale.

In this work, we give a brief overview of the relevant theoretical background of continuum mechanics as well as of the growth and remodelling theory. We demonstrate how this new approach compares with the previous ones for the case of uniaxial tension and extension for pure volume change and pure density change, respectively. Finally, an example of a two-phase material is shown to demonstrate the versatility of this approach. The results are validated against previously published data by Himpel et al. (2005).

2. Methods

2.1 Kinematics

The standard deformation gradient $\mathbf{F}^{\tau}$ is defined as

$$\mathbf{F}^{\tau}(t) = \frac{\partial \mathbf{x}^{\tau}(\mathbf{X}, t)}{\partial \mathbf{X}}, \tag{1}$$

where $\mathbf{x}^{\tau} = \mathbf{x}^{\tau}(\mathbf{X}, t) : \mathcal{B}^{(0,0)} \rightarrow \mathcal{B}^{(\tau,t)}$ is used to describe the

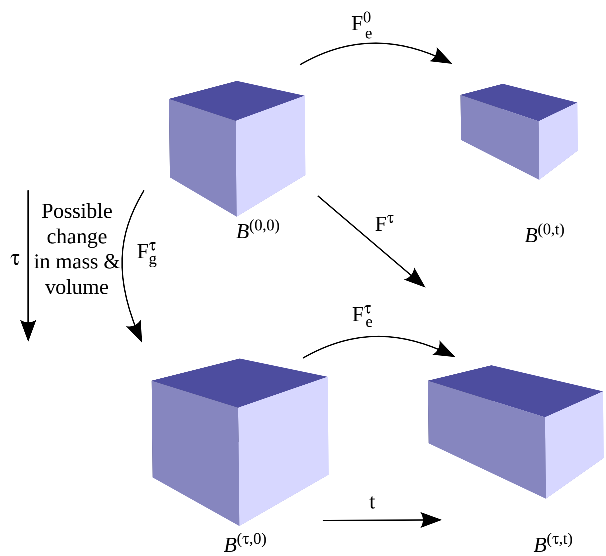

Figure 1. Growth and remodelling and the mechanical equilibrium happen on two different timescales. The timescale t represents the short timescale of *seconds*, whereas τ represents the long timescale in the order of days to months.

deformation between the reference configuration $\mathcal{B}^{(0,0)}$ and the deformed configuration $\mathcal{B}^{(\tau,t)}$ at a given time τ. See Figure 1 for an illustration of the various configurations and timescales. Growth and remodelling and the mechanical equilibrium happen on two different timescales. The timescale t represents the short timescale of *seconds* (mechanical equilibrium), whereas τ represents the long timescale in the order of *days* to *months* (growth and remodelling or material equilibrium), see Figure 1. Note that in most cases, the dependency on the short timescale t is omitted for the sake of simplicity. The deformation gradient may be split into a growth part and an elastic part $\mathbf{F}^{\tau} = \mathbf{F}_{\mathrm{e}}^{\tau}\mathbf{F}_{\mathrm{g}}^{\tau}$ with $J^{\tau} = \det\mathbf{F}^{\tau} > 0$, $J_{\mathrm{e}}^{\tau} = \det\mathbf{F}_{\mathrm{e}}^{\tau} = 1$ and $J_{\mathrm{g}}^{\tau} = \det\mathbf{F}_{\mathrm{g}}^{\tau} > 0$, ensuring the invertibility of those three tensors and the incompressibility of the ground substance. $\mathbf{F}_{\mathrm{g}}^{\tau}$ describes the effect of finite growth (Himpel 2007).

The total right Cauchy–Green tensor $\mathbf{C}^{\tau}$ and the total Green–Lagrange strain tensor $\mathbf{E}^{\tau}$ are defined as follows:

$$\mathbf{C}^{\tau} = (\mathbf{F}^{\tau})^{\mathrm{T}}\mathbf{F}^{\tau} \quad \mathbf{E}^{\tau} = \frac{1}{2}((\mathbf{F}^{\tau})^{\mathrm{T}}\mathbf{F}^{\tau} - \mathbf{I}). \tag{2}$$

Similarly, the elastic right Cauchy–Green tensor $\mathbf{C}_{\mathrm{e}}^{\tau}$ and the elastic Green–Lagrange strain tensor $\mathbf{E}_{\mathrm{e}}^{\tau}$ are defined as follows:

$$\mathbf{C}_{\mathrm{e}}^{\tau} = \left(\mathbf{F}_{\mathrm{e}}^{\tau}\right)^{\mathrm{T}}\mathbf{F}_{\mathrm{e}}^{\tau} \quad \mathbf{E}_{\mathrm{e}}^{\tau} = \frac{1}{2}\left((\mathbf{F}_{\mathrm{e}}^{\tau})^{\mathrm{T}}\mathbf{F}_{\mathrm{e}}^{\tau} - \mathbf{I}\right). \tag{3}$$

2.2 Free energy and stress–strain relationship

The second Piola–Kirchhoff stress tensor $\mathbf{S}^{\tau}$ and its relations to the first Piola–Kirchhoff stress tensor $\mathbf{P}^{\tau}$ and to the Cauchy–stress tensor $\boldsymbol{\sigma}^{\tau}$ are given as follows:

$$\mathbf{S}^{\tau} = J^{\tau}(\mathbf{F}^{\tau})^{-1}\boldsymbol{\sigma}^{\tau}(\mathbf{F}^{\tau})^{-\mathrm{T}} = (\mathbf{F}^{\tau})^{-1}\mathbf{P}^{\tau}. \tag{4}$$

Other authors (Himpel et al. 2005) also introduced the Mandel stresses in the intermediate configuration $\mathcal{B}^{(\tau,\,0)}$, which drive the evolution equation for mass change. In our approach, we will show that utilising the second Piola–Kirchhoff stress tensor gives qualitatively similar results.

Following the principle of material objectivity, the free energy function Ψ^{τ} per unit reference volume may be written as follows:

$$\Psi^{\tau} = \Psi^{\tau}\left(\mathbf{C}_{\mathrm{e}}^{\tau}\right). \tag{5}$$

For the convenient description of growth and remodelling phenomena, we introduce the density prior to growth and remodelling at time $\tau = 0$ as $\rho^{(0,0)}$ in the reference configuration and $\rho^{(0,t)}$ in the current configuration, whereas the densities at later times $\tau = \tau$ are given as $\rho^{(\tau,\,0)}$ in the reference configuration and $\rho^{(\tau,t)}$ in the current configuration. Note that, due to incompressibility, $\rho^{(\tau,t)} = \rho^{(\tau,0)}$, which will be used subsequently. By using those definitions, one can introduce a normalised density and hence a weighted free energy at time τ, with respect to the volume in the reference configuration (Himpel et al. 2005):

$$\Psi^{\tau} = \frac{\rho^{(\tau,0)}}{\rho^{(0,0)}}\Psi^{0}\left(\mathbf{C}_{\mathrm{e}}^{\tau}\right) = \theta^{\tau}\Psi^{0}\left(\mathbf{C}_{\mathrm{e}}^{\tau}\right), \tag{6}$$

where θ^{τ} represents the normalised density at time τ, and we omit the superscript $t = 0$ since θ^{τ} does not change with t. Ψ^{0} represents the free energy before any growth and remodelling has occurred. The stress–strain relationship for an incompressible material then follows as

$$\begin{aligned}\mathbf{S} &= 2\frac{\partial\Psi^{\tau}}{\partial\mathbf{C}^{\tau}} - p(\mathbf{C}^{\tau})^{-1} = \left(\mathbf{F}_{\mathrm{g}}^{\tau}\right)^{-1}\mathbf{S}_{\mathrm{e}}^{\tau}\left(\mathbf{F}_{\mathrm{g}}^{\tau}\right)^{-\mathrm{T}} \\ &= 2\left(\mathbf{F}_{\mathrm{g}}^{\tau}\right)^{-1}\left(\frac{\partial\Psi^{\tau}}{\partial\mathbf{C}_{\mathrm{e}}^{\tau}} - \frac{p}{2}(\mathbf{C}_{\mathrm{e}}^{\tau})^{-1}\right)\left(\mathbf{F}_{\mathrm{g}}^{\tau}\right)^{-\mathrm{T}}.\end{aligned} \tag{7}$$

As mentioned in the introduction, biological tissues may be represented as a composite of $\gamma = 1, \ldots, C$ constituents, and thus the free energy may be written as the sum of the energy of its constituents γ:

$$\Psi^{\tau} = \sum_{\gamma=1}^{C}\theta_{\gamma}^{\tau}\Psi_{\gamma}^{0} \quad \text{with} \quad \theta_{\gamma}^{0} = 1, \quad \forall\gamma. \tag{8}$$

This assumption was motivated by Humphrey and Rajagopal (2002) in the context of a constrained mixture theory. The strain for each constituent is assumed to be the same, and thus the stress–strain relationship for a biological tissue consisting of C constituents reads

$$\mathbf{S} = 2\left(\mathbf{F}_{\mathrm{g}}^{\tau}\right)^{-1}\frac{\partial\Psi^{\tau}}{\partial\mathbf{C}_{\mathrm{e}}^{\tau}}\left(\mathbf{F}_{\mathrm{g}}^{\tau}\right)^{-\mathrm{T}} - p(\mathbf{C}^{\tau})^{-1}$$
$$= 2\sum_{\gamma=1}^{C}\theta_{\gamma}^{\tau}\left(\mathbf{F}_{\mathrm{g}}^{\tau}\right)^{-1}\frac{\partial\Psi_{\gamma}^{0}}{\partial\mathbf{C}_{\mathrm{e}}^{\tau}}\left(\mathbf{F}_{\mathrm{g}}^{\tau}\right)^{-\mathrm{T}} - p(\mathbf{C}^{\tau})^{-1}. \tag{9}$$

Cross-coupling terms for the interaction of different constituents may also be considered. They are omitted in this context, because studies up to date have consistently been able to approximate the complex mechanical response of the composite by neglecting the cross-coupling terms (Gleason and Humphrey 2004; Watton et al. 2004; Holzapfel 2006; Schmid et al. 2010). Refined molecular imaging techniques and mechanical testing procedures may help to improve these descriptions.

2.3 Numerical implementation of incompressibility

If a material does not change its volume under deformation, it is said to be incompressible. This property can be captured by the following equation:

$$\det\left(\mathbf{F}_{\mathrm{e}}^{\tau}(t)\right) = 1 \quad \text{throughout the deformation, i.e.} \quad \forall t \text{ with } 0 < t \leqslant \tau. \tag{10}$$

Numerically, this is considered via two independent fields in the FE formulation: the nodal displacements and the hydrostatic pressure field, e.g. Bathe (1982) and Nash and Hunter (2000). These are the so-called hybrid or $u - p$ formulations. Care should be taken to underintegrate the hydrostatic pressure field to avoid locking phenomena (Oden 1972). To reflect that, volume does not change; the kinematic constraint (Equation (10)) is incorporated over each element with volume V_{elem} into the global system (Nash and Hunter 2000):

$$\int_{V_{\mathrm{elem}}}(\det\left(\mathbf{F}_{\mathrm{e}}^{\tau}\right) - 1)\mathrm{d}V, \tag{11}$$

where $\det\left(\mathbf{F}_{\mathrm{e}}^{\tau}\right)$ is the standard Jacobian of the deformation gradient tensor on the short timescale when no volume or mass change occurs. Equation (11) offers the opportunity for seemlessly enforcing the changing volume.

2.4 Growth and remodelling

Growth and remodelling describe the biological process of adaptation as illustratively summarised by Taber (1995). For example, in an aneurysm – a pathological dilatation of the arterial wall – apoptosis[2] of vascular smooth muscle cells in the medial layer is accompanied by a substantial loss of elastin and collagen (Anidjar and Kieffer 1992; Kondo et al. 1997). To be able to describe such phenomena within the same FE environment, we briefly introduce some basic notions of density, volume and volume fractions ensuring a consistent handling of these properties, see also Ateshian et al. (2009) and Ehlers et al. (2009). This is done first for one constituent and subsequently generalised to several constituents.

2.4.1 One constituent

For one constituent, we introduce the infinitesimal[3] mass m, the infinitesimal volume $\mathrm{d}V$ and the infinitesimal density $\rho = m/\mathrm{d}V$. Those measures may, of course, depend on time and differ for $\tau = 0$ and $\tau = \tau$:

$$\rho^{0}, m^{0}, \mathrm{d}V^{0} \quad \text{and} \quad \rho^{\tau}, m^{\tau}, \mathrm{d}V^{\tau}. \tag{12}$$

Next, we introduce the normalised mass change:

$$f^{\tau} = \frac{m^{\tau}}{m^{0}} = \frac{\rho^{\tau}\mathrm{d}V^{\tau}}{\rho^{0}\mathrm{d}V^{0}} = \theta^{\tau}\nu^{\tau}, \tag{13}$$

where $\theta^{\tau} = (\rho^{\tau}/\rho^{0})$ and $\nu^{\tau} = (\mathrm{d}V^{\tau}/\mathrm{d}V^{0})$ are the normalised density change and normalised volume change,[4] respectively. Note that the word 'normalised' refers to the fact that for $\tau = 0$, all normalised variables have value 1. It can be considered as a normalisation with respect to a time when no density or volume change has occurred, i.e. the tissue is in a virgin state one wants to refer to. Additionally, the normalised volume change v^{τ} (defined on the timescale τ) is not the volume change usually defined by the determinant of the elastic deformation gradient $\det(\mathbf{F}_{\mathrm{e}})$ which is determined by the short timescale t.

2.4.1.1 Pure volume change. For pure volume change, $\theta^{\tau} = 1, \forall\tau$ and $f^{\tau} = v^{\tau}$. This is used to govern the incompressibility condition:

$$\det(\mathbf{F}^{\tau}) - \nu^{\tau} = 0, \tag{14}$$

which yields an adapted volume according to the mass change at time τ. The constitutive Equation (6) remains unaffected, since $\theta^{\tau} = 1, \forall\tau$.

2.4.1.2 Pure density change. For pure density change, $v^{\tau} = 1, \forall\tau$ and $f^{\tau} = \theta^{\tau}$. Thus, the incompressibility condition remains unchanged, whereas the constitutive equation changes over time as defined in Equation (6).

2.4.1.3 Evolution equations. In pure volume change and pure density change, the mass changes due to different mechanisms. In pure volume change, the evolution equation for f^{τ} thus represents a change in volume, whereas for pure density change, f^{τ} represents a change in density. Thus, the same variable has different meanings in those differing contexts. Those mechanisms are the representatives for the different types of biological tissue.

Density changes tend to happen predominantly in hard tissues like bone (Wolff 1892; Huiskes et al. 1987; Kuhl et al. 2003; Taylor et al. 2009), whereas volume change tends to happen predominantly for soft tissues like connective tissue and muscles (Richter and Kellner 1963; Humphrey 2002; Hu et al. 2007).

Equation (15) introduces the general form of an evolution equation for the mass change or equivalently for the normalised mass change:

$$\begin{aligned} &\frac{\mathrm{d}m^{\tau}}{\mathrm{d}\tau} = \mathcal{F}(\alpha, E, S) \quad \text{or equivalently} \\ &\frac{\mathrm{d}f^{\tau}}{\mathrm{d}\tau} = \tilde{\mathcal{F}}(\alpha, E, S), \end{aligned} \tag{15}$$

where α, E and S are some time constants, kinematic variables or stress variables, respectively. It is not clear which mechanical quantity is driving changes in growth and remodelling. An excellent review about what cells actually sense: 'Stress or strain?' can be found in Humphrey (2001). For example, fibre realignment is thought to be driven by either stress or strain (Driessen et al. 2003, 2004, 2005; Alastrue et al. 2009; Menzel and Waffenschmidt 2009; Grytz and Meschke 2010; Grytz et al. 2010). Previous theoretical investigations which use the split of the deformation gradient into a growth part and elastic part (Cowin 1996; Kuhl et al. 2006; Himpel 2007; Himpel et al. 2005, 2007; Kuhl and Holzapfel 2007; Menzel 2007) suggest the Mandel stress in the intermediate configuration to drive the evolution equation. However, other authors have used the Cauchy stress (Driessen et al. 2003) or the Green strain (Watton et al. 2004, 2009; Schmid et al. 2010) to drive the evolution equation. As noted in Equation (15), the functional form of the evolution equation may thus, in general, depend on both stress and strain. The specific functional form is usually phenomenological, and different linear and nonlinear forms have been suggested and investigated (Taber 2008; Watton et al. 2009; Göktepe et al. 2010).

2.4.2 *Several constituents: illustrative examples*

For several constituents, the equations for mass, volume and density have to be considered for the whole tissue as well as for each constituent (Humphrey and Rajagopal 2002; Garikipati et al. 2004; Ehlers et al. 2009). Based on the previous section, they can be readily derived as follows. Assuming that a material consists of $\gamma = 1, \ldots, C$ constituents, the total density ρ, the partial density of a constituent ρ_γ and the true or individual density of a constituent r_γ are defined as follows:

$$\begin{aligned} &\rho = \frac{m}{\mathrm{d}V}, \\ &m: \text{total mass},\ \mathrm{d}V: \text{ total volume} \\ &\rho_\gamma = \frac{m_\gamma}{\mathrm{d}V}, \\ &m_\gamma: \text{ partial mass of constituent } \gamma \\ &r_\gamma = \frac{m_\gamma}{\mathrm{d}V_\gamma}, \\ &\mathrm{d}V_\gamma: \text{ partial volume of constituent } \gamma. \end{aligned} \tag{16}$$

Furthermore, we define the volume fraction ϕ_γ of a constituent γ as follows:

$$\phi_\gamma = \frac{\mathrm{d}V_\gamma}{\mathrm{d}V}, \tag{17}$$

which combined with Equation (16) implies that

$$\rho_\gamma = \phi_\gamma r_\gamma. \tag{18}$$

Introducing the large timescale τ as a superscript indicates that the above quantities may be changing over time.

Although it is easy to distinguish the two cases of volume change and density change for one constituent, it is reasonable to assume that in reality both mechanisms are observed on a tissue level for composite materials. On a constituent level for soft tissues, it is more likely that volume change is dominant as, for example in myocardial hypertrophy and hyperplasia, muscle mass increases substantially via a change in volume (Taber 2001). Nevertheless, it may be possible for soft tissues to change true densities as well. However, large changes seem to be unlikely because, for example for collagen, an increase in fibril diameter is associated with a decrease in fibril density (Sanders and Goldstein 2001; Sturgis et al. 2002). The true density thus seems to remain nearly constant. Similarly in pathological arterial adaptation like aneurysm formation, the medial elastin tends to completely disappear and with it all other relevant constituents (Kondo et al. 1997). Thus, for the sequel, we assume that for composite materials, the true densities of each constituent remain unchanged ($r^\tau_\gamma = r^0_\gamma$)), whereas volume fractions are allowed to adapt.

Motivated by the concepts introduced by other authors such as Watton et al. (2004, 2009), Kim et al. (2009) and Schmid et al. (2010), we introduce a new variable: the normalised partial mass change of constituent γ:

$$\begin{aligned} &f^\tau_\gamma = \frac{m^\tau_\gamma}{m^0_\gamma} = \frac{r^\tau_\gamma \mathrm{d}V^\tau_\gamma}{r^0_\gamma \mathrm{d}V^0_\gamma} = \underbrace{\zeta^\tau_\gamma}_{=1} \nu^\tau_\gamma = \nu^\tau_\gamma \quad \text{with} \\ &f^0_\gamma = 1, \forall \gamma, \end{aligned} \tag{19}$$

where ζ^τ_γ and ν^τ_γ are the normalised true density change (which is unity) and the normalised partial volume change, respectively. With this, we define the normalised tissue volume change v^{τ} as follows:

$$\nu^{\tau} = \frac{\mathrm{d}V^{\tau}}{\mathrm{d}V^{0}} = \frac{1}{\mathrm{d}V^{0}} \sum_{\gamma=1}^{C} \mathrm{d}V_{\gamma}^{\tau} = \sum_{\gamma=1}^{C} \frac{\mathrm{d}V_{\gamma}^{\tau}}{\mathrm{d}V^{0}} = \sum_{\gamma=1}^{C} \frac{\mathrm{d}V_{\gamma}^{\tau}}{\mathrm{d}V_{\gamma}^{0}} \frac{\mathrm{d}V_{\gamma}^{0}}{\mathrm{d}V^{0}} = \sum_{\gamma=1}^{C} \nu_{\gamma}^{\tau} \phi_{\gamma}^{0} = \sum_{\gamma=1}^{C} f_{\gamma}^{\tau} \phi_{\gamma}^{0}. \tag{20}$$

Note that v^{τ} does not need to remain unity over time τ. It is now possible to compute the changing normalised density from Equation (6) with the help of Equation (19) as follows:

$$\theta_{\gamma}^{\tau} = \frac{\rho_{\gamma}^{\tau}}{\rho_{\gamma}^{0}} = \frac{r_{\gamma}^{\tau} \phi_{\gamma}^{\tau}}{r_{\gamma}^{0} \phi_{\gamma}^{0}} = \frac{\phi_{\gamma}^{\tau}}{\phi_{\gamma}^{0}} = \frac{\mathrm{d}V_{\gamma}^{\tau}}{\mathrm{d}V_{\gamma}^{0}} \frac{\mathrm{d}V^{0}}{\mathrm{d}V^{\tau}} = \nu_{\gamma}^{\tau} \frac{1}{\nu^{\tau}} = f_{\gamma}^{\tau} \frac{1}{\nu^{\tau}}. \tag{21}$$

For the sake of clarity, the important Equations (8,14,20,21) are displayed in a table. Note that the normalised partial mass change f_{γ}^{τ} connects the kinematic with the constitutive level.

Kinematic level	$\int_V (\det(\mathbf{F}^{\tau}) - \nu^{\tau})\mathrm{d}V = 0$	$\nu^{\tau} = \sum_{\gamma=1}^{C} f_{\gamma}^{\tau} \phi_{\gamma}^{0}$
Constitutive level	$\Psi^{\tau} = \sum_{\gamma=1}^{C} \theta_{\gamma}^{\tau} \Psi_{\gamma}^{\tau}$	$\theta_{\gamma}^{\tau} = f_{\gamma}^{\tau} 1/\nu^{\tau}$

When several constituents are present in a tissue and the assumption holds that the true density remains constant, one may, nevertheless, observe pure volume or pure density change as well as volume and density change on the tissue level. This depends on the evolution equations and the choice of parameters. Table 1 depicts the initial configuration at time $\tau = 0$ and three different cases illustrating the effect on the above-introduced variables.

2.5 *Numerical implementation*

The introduced formalism for modelling adaptation in the FE environment was implemented in the FE code CMISS (www.cmiss.org) as introduced in detail by Nash and Hunter (2000). The code handles arbitrary biomechanical problems in three dimensions for large deformation mechanics.

2.6 *Evolution equations*

The derivations of the evolution equations in Himpel et al. (2005) are based on thermodynamic considerations for internal variables. Biological tissues, however, are thermodynamically open systems, and thus phenomenological evolution equations for the normalised mass change f_{γ}^{τ} may also be based on experimental observations. This has the possible advantage that variables for the evolution equations and thus the related quantities mass fraction or volume fractions may be traced experimentally over time (Fisher and Llaurado 1966; Rizzo et al. 1989; Gleason and Humphrey 2004).

For a conceptual proof of our model, we utilise the following evolution concept motivated by previous experimental observations (Takamizawa and Hayashi 1987, 1988). In this approach, we apply the concept of 'homeostatic equilibrium' and express the evolution of the normalised partial mass change through an ordinary differential equation. First, a so-called homeostatic stress

Table 1. This table depicts a tissue originally consisting of two constituents A and B which have the same volume fraction. Three different cases are shown and the corresponding values of the above-introduced relevant parameters for adaptation are given.

			f_γ	V_γ	ϕ_γ	m_γ	ρ_γ	r_γ	θ_γ
Reference cube 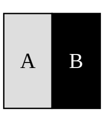	$\tau = 0$								
	$V^0 = 1$	$\gamma = A$	1	1/2	1/2	2	2	4	1
	$\nu^0 = 1$	$\gamma = B$	1	1/2	1/2	3	3	6	1
(1) Volume change 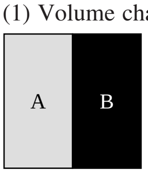	$\tau = \tau^*$		f_γ	V_γ	ϕ_γ	m_γ	ρ_γ	r_γ	θ_γ
	$V^{\tau^*} = 2$	$\gamma = A$	2	1	1/2	4	2	4	1
	$\nu^{\tau^*} = 2$	$\gamma = B$	2	1	1/2	6	3	6	1
(2) Density change 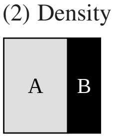	$\tau = \tau^*$		f_γ	V_γ	ϕ_γ	m_γ	ρ_γ	r_γ	θ_γ
	$V^{\tau^*} = 1$	$\gamma = A$	4/3	2/3	2/3	8/3	8/3	4	4/3
	$\nu^{\tau^*} = 1$	$\gamma = B$	2/3	1/3	1/3	2	2	6	2/3
(3) General case 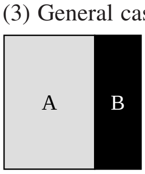	$\tau = \tau^*$		f_γ	V_γ	ϕ_γ	m_γ	ρ_γ	r_γ	θ_γ
	$V^{\tau^*} = 2$	$\gamma = A$	8/3	4/3	2/3	16/3	8/3	4	4/3
	$\nu^{\tau^*} = 2$	$\gamma = B$	4/3	2/3	1/3	4	2	6	2/3

Note that it is very likely for a soft tissue to observe the general case, because for case (1) and case (2) rate equations and thus the change in the partial volumes need to have very specific values.

($\mathbf{S}_h$) or strain ($\mathbf{E}_h$) under a given load is being determined before any adaptation takes place ($\tau = 0$). Second, this is used as a 'target stress' tr($\mathbf{S}_h$) or 'target strain' tr($\mathbf{E}_h$) for the rest of the adaptation [5] and leads, in the simplest case, to the following equations:

$$\frac{\mathrm{d}f_\gamma^\tau}{\mathrm{d}\tau} = \alpha_S \frac{\mathrm{tr}(\mathbf{S}_{\mathrm{cur}}) - \mathrm{tr}(\mathbf{S}_{\mathrm{h}})}{\mathrm{tr}(\mathbf{S}_{\mathrm{h}})} \quad \text{or} \quad \text{similarly} \qquad \frac{\mathrm{d}f_\gamma^\tau}{\mathrm{d}\tau} = \alpha_E \frac{\mathrm{tr}(\mathbf{E}_{\mathrm{cur}}) - \mathrm{tr}(\mathbf{E}_{\mathrm{h}})}{\mathrm{tr}(\mathbf{E}_{\mathrm{h}})}. \tag{22}$$

The variables α_E and α_S are the respective rate constants. This approach has been generalised from a 1D approach for embedded collagen fibres within a matrix (Watton et al. 2004, 2009; Schmid et al. 2010).

2.7 Simulations

To validate the consistent formulation presented herein, we investigated different cases for a unit cube ($1\,\mathrm{cm}^3$) with a Neo–Hookean material response. Firstly, we investigated the case of pure volume change for one constituent, i.e. a constant density throughout the adaptive process. This was done for uniaxial extension with step increases in the displacement. Secondly, the case of pure density change is presented for a unit cube under uniaxial tension with step increases in force. For effortless validation, the material parameters and the geometry were adopted from Himpel et al. (2005) and are listed in Table 2. Note, however, that they used a compressible version of the Neo–Hookean response such that material parameters differ to ensure similar stress responses. For isotropic growth, the growth tensor is $\mathbf{F}_g^\tau = \lambda_g \mathbf{I}$. Considering that $\lambda_g = v^{1/3}$, we have

$$\Psi^\tau = \frac{1}{2}\theta^\tau k\left(\mathrm{tr}\left(\mathbf{C}_e^\tau\right) - 3\right), \tag{23}$$

and, thus

$$\begin{aligned}\mathbf{S} &= 2\left(\mathbf{F}_g^\tau\right)^{-1}\frac{\partial\Psi^\tau}{\partial\mathbf{C}_e^\tau}\left(\mathbf{F}_g^\tau\right)^{-\mathrm{T}} - p(\mathbf{C}^\tau)^{-1} \\ &= 2\nu^{-2/3}\frac{\partial\Psi^\tau}{\partial\mathbf{C}_e^\tau} - p(\mathbf{C}^\tau)^{-1} \\ &= \nu^{-2/3}\theta^\tau k\mathbf{I} - p(\mathbf{C}^\tau)^{-1}.\end{aligned} \tag{24}$$

Lastly, a unit cube consisting of two different constituents is investigated under uniaxial extension to illustrate the advantage of this approach, i.e. being able to validate volume or mass fractions at different times during the adaptation process.

3. Results

3.1 Pure volume change

Following Himpel et al. (2005), we used uniaxial extension tests of a unit cube to show the validity of pure volume change for one constituent. For physiologically realistic adaptation, the tissue was first stretched up

Table 2. This table lists the material parameters for all five simulations.

	Pure volume change	Pure density change	Composite change case 1		Composite change case 2a		Composite change case 2b	
			A	B	A	B	A	B
Constituent	0.1	–	0.1		0.1		0.1	
Δu_x in (cm)	–							
ΔF_x in (N)		4.0	–	–	–	–	–	–
Adaptation type	tr(**S**)	tr(**E**)	tr(**S**)		tr(**S**)		tr(**S**)	
k(Pa)	0.169	169.2	1.0	5.0	1.0	5.0	5.0	1.0
Time step (time unit)	1.0	1.0	1.0		1.0		1.0	
Remodelling								
α_E (1/time unit)	–	0.15	–	–	–	–	–	–
Tr($\mathbf{E}_h$) (no unit)	–	4.2E − 02	–	–	–	–	–	–
α_S (1/time unit)	0.05	–	0.15	–	0.15	–	–	0.15
Tr($\mathbf{S}_h$) (Pa)	9.5E − 06	–	1.492	–	1.492	–	–	1.492
Degradation								
$b_{\min}$ (no unit)	–	–	0.1	–	–	0.5	0.5	–
$\hat{\tau}$ (time unit)	–	–	100	–	–	150	150	–

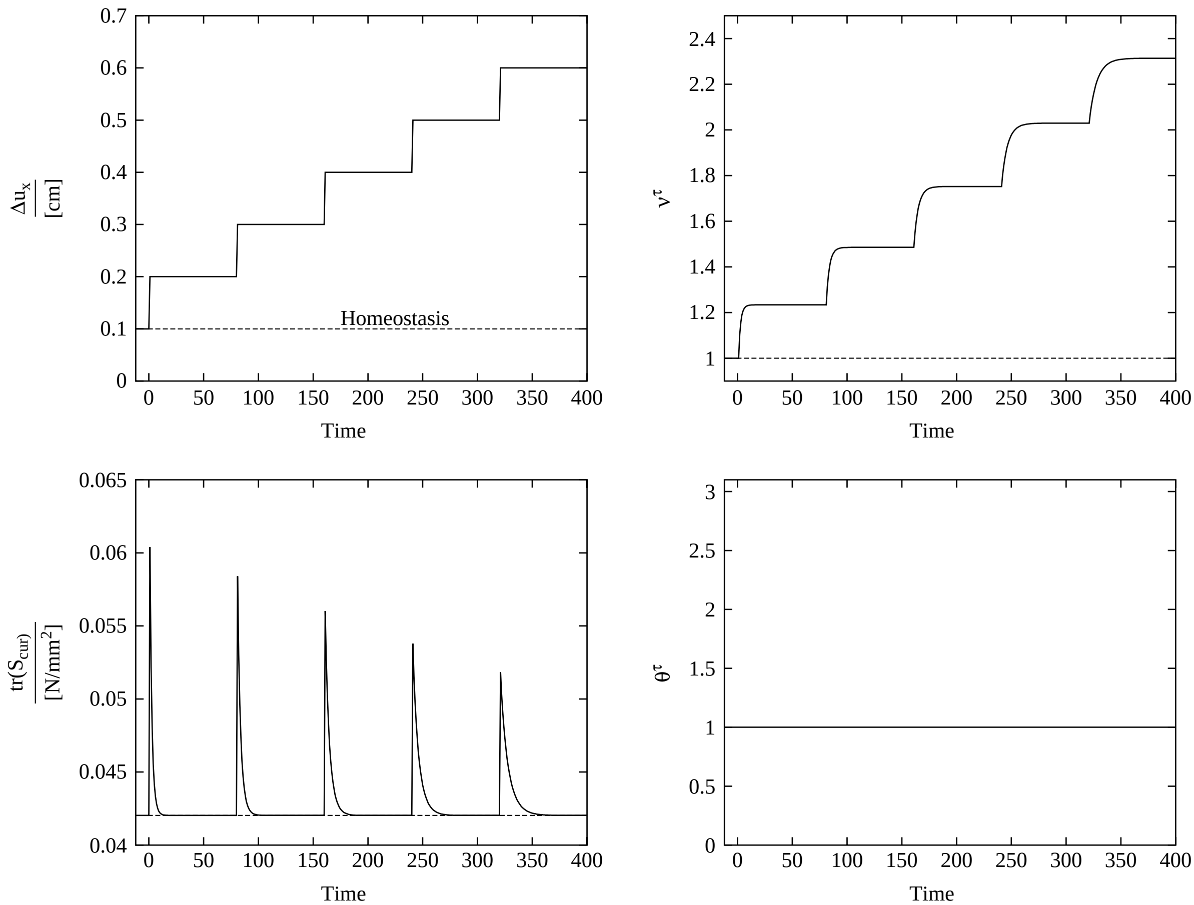

Figure 2. Pure volume change. The graphs depict the prescribed time course of steps in the displacement (top left), the resulting relative volume change with respect to the original volume (top right), the changes in the trace of the stress which, as determined by the evolution equation, tends to go back to its original value (bottom left) and the normalised density which remains unity (bottom right).

to a '*homeostatic*' stretch of $\lambda_x = \lambda_\mathrm{h} = 1.1$ in which the quantity $\mathrm{tr}(\mathbf{S})$ was taken as a point of reference for subsequent axial adaptation steps. Additional displacements of $\Delta u_x = 0.1$ cm were applied five times up to a final value of $\lambda_x = 1.6$, $u_x = 0.6$ cm.

The graphs show excellent agreement with the data from Himpel et al. (2005) (Figure 6) for the case where the stretch limit is not reached ($\vartheta^+ = 2.00$). Note that (Figure 2, top right) with progressive displacement steps, the difference in the limit values of the relative volume change between two successive steps increases. Although the displacement steps have the same value each time, the volume increases with cubic power ($\Delta v^\tau \sim (\Delta u)^3$).

3.2 Pure density change

To show that the concept of 'homeostatic equilibrium' holds for the case of a single constituent with pure density change as well, we followed Himpel et al. (2005) and used uniaxial tension tests of a unit cube for one constituent. For physiologically realistic adaptation, the tissue was first loaded up to a '*homeostatic*' load of $F_x = F_\mathrm{h} = 4.0$ N in which the quantity[6] $\mathrm{tr}(\mathbf{E}_\mathrm{h})$ was taken as a point of reference for subsequent axial adaptation steps. Additional loads of $\Delta F_x = 4.0$ N were applied five times up to a final value of 20.0 N.

The graphs in Figure 4 show excellent agreement with the data from Himpel (2007) (Figure 3.2) for the case when the material is assumed to be incompressible. It can be concluded that the concept of 'homeostatic equilibrium' is an appropriate alternative to model adaptation (Figure 3).

3.3 Density and volume change

As an illustrative example, we take a tissue which consists of two constituents A and B. The value of the constitutive parameter k of the Neo–Hookean material is taken to be different for both constituents (Figure 4). We consider two different types of loading:

Case 1. *One load step*: the first one is used to illustrate the systemic effects of coupling the degradation of one constituent and the adaptation of another. For this, we introduce two constituents A and B with material

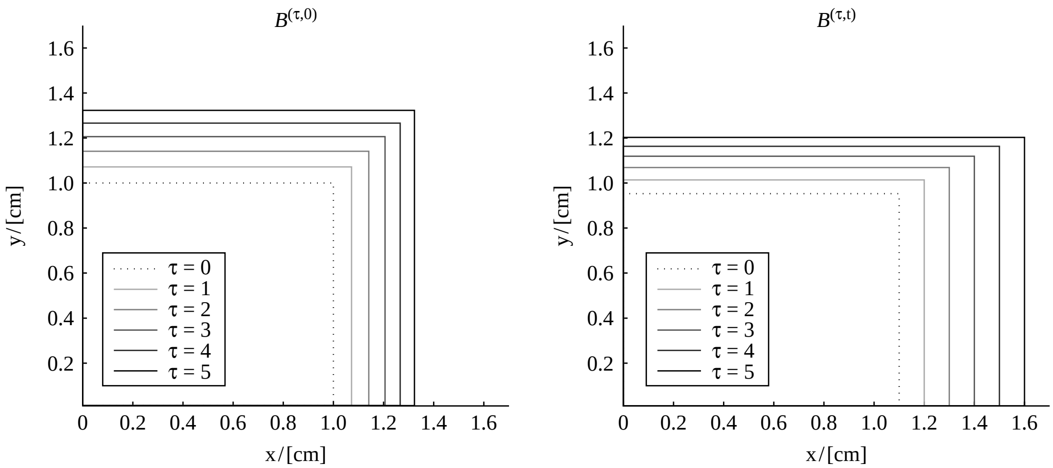

Figure 3. Evolution of reference and current configuration. The left image shows the evolution of the reference configuration. The evolution of this cube is due to changing reference volume $\mathrm{f} > \nu^{\tau}$, cf. Equation (14) and is described by the growth deformation tensor $\mathbf{F}_{\mathrm{g}}^{\tau}$. The right image shows the evolution of the current configuration due to increased displacement boundary conditions and a change in the reference configuration. Note that the cross-sectional area is rectangular in the current configuration because of the applied axial stretch.

parameters $k_{A_1} = 1$ and $k_{B_1} = 5$. The initial volume fractions of both constituents are taken to be $\phi_A^0 = \phi_B^0 = 0.5$. The tissue is initially stretched in the axial direction to a '*homeostatic value*' of $\lambda_x = \lambda_{\mathrm{h}} = 1.1$. Subsequently, constituent B is being degraded via $f_B(\tau) = b_{\min}^{\tau/\hat{\tau}}$, where $\hat{\tau}$ is the time at which f_B reaches the value $b_{\min}$. Constituent A, on the other hand, is allowed to adapt according to the evolution Equation $(22)_2$.

Note that the current trace of the stress $\mathrm{tr}(\mathbf{S}_{\mathrm{cur}})$ initially overshoots the target stress $\mathrm{tr}(\mathbf{S}_{\mathrm{h}})$, yet eventually reaches it. This pattern could be interpreted as a phenomenon which (Bellousov 1998; Taber 2008) is described as the hyper-restoration law. This simulation suggests that it might be a systemic effect of one constituent degrading and the other substituting its function. Note this is also due to the choice of rate constants, i.e. that constituent B is degrading faster than constituent A can adapt. If this was to be vice versa, no overshoot would occur. Furthermore, both the volume and the density adapt over time, so that on a tissue level, one cannot consider it to be either pure volume or pure density change.

Case 2. *Several load steps*: we distinguish two different scenarios with $k_{A_{2a}} = 1$ and $k_{B_{2a}} = 5$ and with $k_{A_{2b}} = 5$ and $k_{B_{2b}} = 1$. The initial volume fractions of both constituents are taken to be $\phi_A^0 = \phi_B^0 = 0.5$ for both cases. The tissue is initially stretched in the axial direction to a '*homeostatic value*' of $\lambda_x = \lambda_{\mathrm{h}} = 1.1$. In subsequent time steps, constituent B is being degraded via $f_B(\tau) = b_{\min}^{\tau/\hat{\tau}}$, where $\hat{\tau}$ is the time at which f_B reaches its target value $b_{\min}$. Constituent A, on the other hand, is allowed to adapt according to the evolution Equation $(22)_2$ (Figure 5).

It can be seen that, as predicted, both phenomena of volume change and density change actually take place on a tissue level, if the material consists of several components. In Case 2a, the material that is being degraded (A) is weaker than the one that is adapting (B) ($k_A < k_B$), whereas it is the other way around for Case 2b ($k_B < k_A$). Therefore, it is expected that in Case 2a, less material of constituent B is needed to compensate for the stiffness loss of material A than in Case 2b, which can be seen by comparing both the relative volume and relative density changes in Figures 6 and 7. Although the relative volume change in Figure 7 is monotonically increasing for each displacement step, the relative volume change in Figure 6 has an inflection point for each displacement step, because the material B with higher material stiffness takes over a major part of the load and thus less material is needed. For increasing load steps, most of the whole material is made of material B, and thus the inflection point becomes less and less prominent.

4. Discussion

4.1 Heterogeneities

Densities of constituents tend to be vastly heterogeneous throughout a given volume of soft tissues (Sands et al. 2005; Pope et al. 2008; Kim et al. 2009). It is thus important that local changes in mass can be handled on a Gauss point basis in the FE model, which has been implemented in this code. In this way, the remodelling equations can account for local stress and strain heterogeneities and their effects on the growth and remodelling processes. This was used in the context of pure density change for arterial adaptation (Schmid et al. 2010).

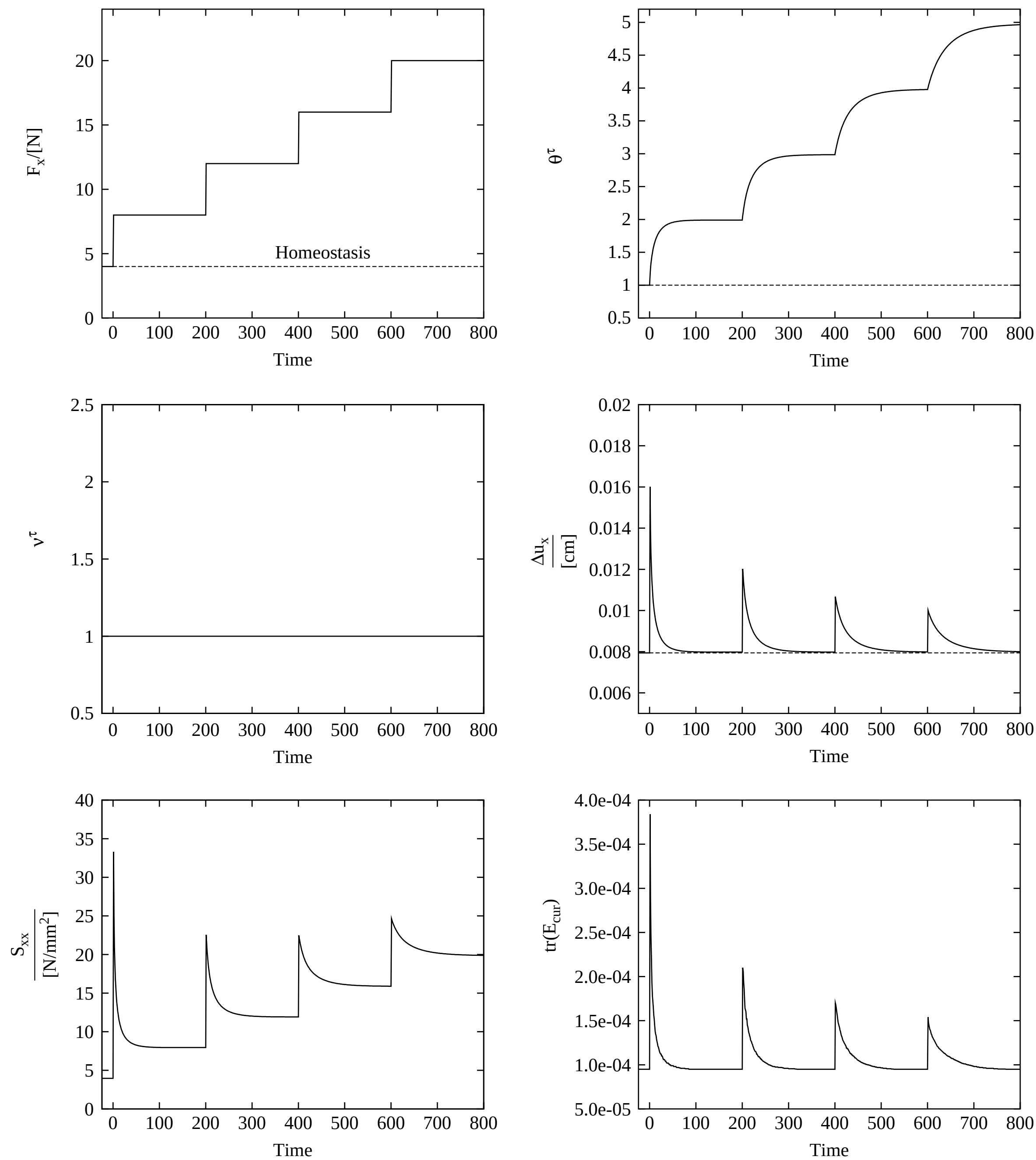

Figure 4. Pure density change. The graphs depicts the prescribed time course of steps in the axial force (top left), the resulting normalised density with respect to the original density (top right), the normalised volume which remains unity (middle left) and the changes in the displacement which, as determined by the evolution equation, tends to go back to its original value (middle right). The second Piola–Kirchhoff stress in the *x*-direction (bottom left) is increasing over time, because the axial force is increasing as well. The target strain is reached for each step increase in the force (bottom right).

4.2 Connection between type of adaptation and driving term in the evolution equation

Section 2.4.1.1 points out that in the case of pure volume change, the variable $f^\tau = \nu^\tau$ and is thus a kinematic variable. In Section 2.4.1.2, on the other hand, the variable $f^\tau = \theta^\tau$ and is thus a variable which acts by weighting the stress. In Section 3.1, the driving term for pure volume change is chosen to be tr(**S**), whereas in Section 3.2, the driving term is tr(**E**). Thus, the energetically conjugate variables need to be used to ensure convergence.

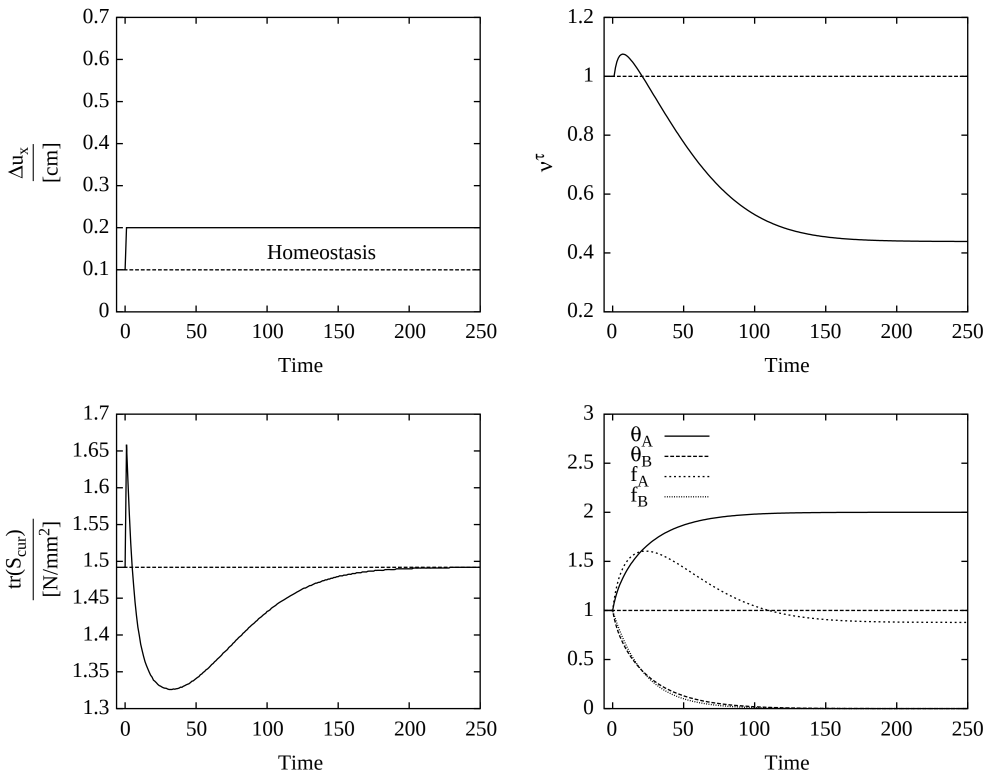

Figure 5. Two constituents, Case 1. The graphs depict the prescribed time course of the load step in the axial displacement (top left), the resulting tissue volume changes with respect to the original volume (top right), the current trace of the stress $\mathrm{tr}(\mathbf{S}_{cur})$ (bottom left) and the normalised density and the mass change (bottom right) of both constituents. Note that the current trace of the stress $\mathrm{tr}(\mathbf{S}_{cur})$ initially overshoots the target stress $\mathrm{tr}(\mathbf{S}_h)$ yet eventually reaches it.

This is also reflected in the type of boundary condition used for those two examples.

4.3 Evolution equations

The introduced evolution equation is linear in its form and thus represents the simplest case. According to Bellous-sov's hyper-restoration hypothesis, tissue responses to stress perturbations tend to restore, but initially overshoot, the original (target) stress (Bellousov 1998; Taber 2008). Our simulation suggests that this effect may be due to a systemic effect of degradation and adaptation playing in concert to reach a given target stress value. Stress overshoot could also be obtained by letting the target stress change at a rate proportional to the same stress difference (Taber 2008). This was done for 1D evolution equations and may serve as a possible mechanism to expand the above-introduced evolution equations to three dimensions.

Furthermore, higher order strain or stress invariants may be used to capture the underlying material symmetry. Further investigations are necessary to clarify the connection between phenomenological descriptions of one and several constituents.

4.4 Incompressibility

The condition of incompressibility may be enforced differently as well, via split of the deformation gradient into a volumetric and a deviatoric part (Ogden 1997; Holzapfel 2000). The volumetric part is chosen to be up to 100–1000 times stiffer than the deviatoric part, ensuring the required property. The stress–strain relationship does then contain the Lagrange multiplier p. This is also called near incompressibility, alluding to the fact that in reality no material is absolutely incompressible. For more theoretical details and numerical implementations, please refer to Peng and Chang (1997) and Hartmann and Neff (2003).

4.5 Summary

We have presented a formulation for tissue adaptation which is consistent on the kinematic and constitutive level. This method utilises the fact that incompressibility and volume growth happen on substantially different time-scales. This approach has the advantage that it can be validated against physiological measurements of volume or mass fractions, see, e.g. Rizzo et al. (1989). It was validated against previous numerical simulations

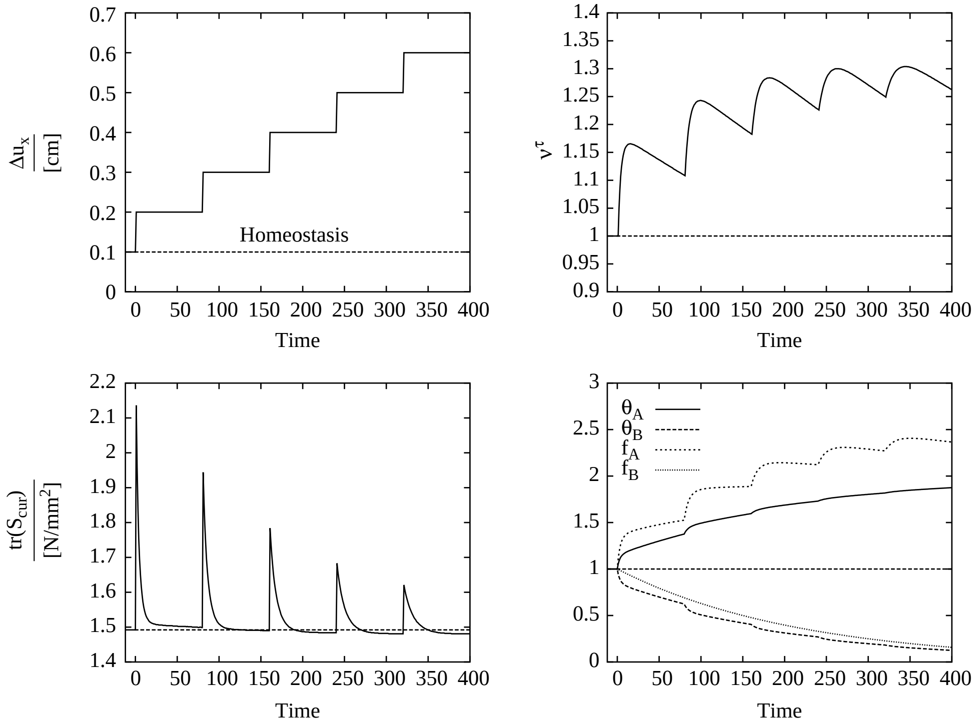

Figure 6. Two constituents, Case 2a. The graphs depict the prescribed time course of steps in the axial displacement (top left), the resulting tissue volume changes with respect to the original volume (top right), the current trace of the stress tr($\mathbf{S}_{cur}$) (bottom left) and the normalised density and the mass change (bottom right). Note that the tissue volume decreases although the target stress seems to be reached after approximately 80 time steps. As a matter of fact, the target stress is not reached as illustrated in Case 1, which is why the volume is still decreasing. Another load step then interferes with this overshoot so it cannot be discerned.

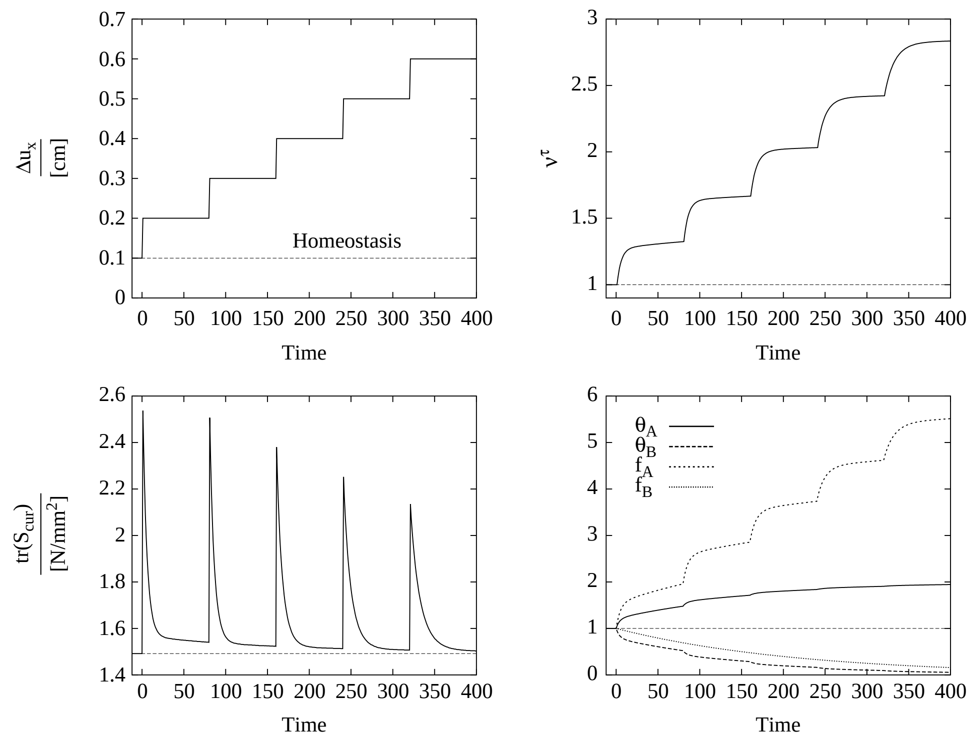

Figure 7. Two constituents, Case 2b. The graphs depict the prescribed time course of steps in the axial displacement (top left), the resulting relative volume change with respect to the original volume (top right), the current trace of the stress tr($\mathbf{S}_{cur}$) (bottom left) and the normalised density and the mass change (bottom right).

(Himpel et al. 2005) and thus holds promise for simple implementations in future studies.

Notably, the effect of hyper-restoration (Bellousov 1998; Taber 2008) seems to be a consequence of a systemic effect of different constituents degrading and adapting at different rates.

Acknowledgements

The authors would like to thank Alexander Gnech, Christian Krawzyk and Simo Schmidt from RWTH Aachen University for the support in validating the code; also we would like to acknowledge Prof. Peter Hunter from the Auckland Bioengineering Institute for making the source code of CMISS available. Furthermore, helpful discussions with Dr Paul Watton from Oxford University are gratefully acknowledged.

Notes

1. Migration of cells within the tissue would be a possible contribution to the convective term, yet would also happen on a longer timescale.
2. Programmed cell death by inflammatory molecules.
3. We neglect the word infinitesimal in the sequel.
4. Note that this fraction is not a derivative but the division of two infinitesimal volumes at different times. The infinitesimal d is upright, whereas the differential *d* is slanted.
5. The first invariant was chosen for the sake of simplicity. Experimental guidance is necessary to further qualify the dependence on possibly other invariants and possible nonlinear dependencies.
6. Himpel et al. (2005) used a range of values for the so-called stress stimulus attractor (Beaupre et al. 2005). In our approach, using the target strain quantity $\mathrm{tr}(\mathbf{E}_h)$ to be the homeostatic one, equates to setting the stress stimulus attractor to zero.

References

Alastrue V, Martinez MA, Doblare M, Menzel A. 2009. Anisotropic micro-sphere-based finite elasticity applied to blood vessel modelling. J Mech Phys Solids. 57(1):178–203.

Anidjar S, Kieffer E. 1992. Pathogenesis of acquired aneurysms of the abdominal aorta. Ann Vasc Surg. 6:298–305.

Ateshian GA, Costa KD, Azeloglu EU, Morrison B, III, Hung CT. 2009. Continuum modeling of biological tissue growth by cell division, and alteration of intracellular osmolytes and extracellular fixed charge density. J Biomech Eng. 131: 1–12.

Bathe KJ. 1982. Finite element procedures. Upper Saddle River, NJ: Prentice-Hall, Inc.

Beaupre GS, Orr TE, Carter DR. 2005. An approach for time-dependent bone modeling and remodeling-theoretical development. J Orthop Res. 8:651–661.

Bellousov LV. 1998. The dynamic architecture of a developing organism: an interdisciplinary approach to the development of organisms. Dordrecht: Kluwer.

Carter DR, Hayes WC. 1977. The compressive behaviour of bone as a two-phase porous structure. J Bone Joint Surg. 59-A7: 175–193.

Cowin SC. 1996. Strain or deformation rate dependent finite growth in soft tissues. J Biomech. 29:647–649.

Cowin SC, Hegedus DH. 1976. Bone remodeling 1: theory of adaptive elasticity. J Elasticity. 6(3):313–326.

Driessen NJB, Bouten CVC, Baaijens FPT. 2005. A structural constitutive model for collagenous cardiovascular tissues incorporating the angular fiber distribution. J Biomech Eng. 127:494–504.

Driessen NJB, Peters GWM, Huyghe JM, Bouten CVC, Baaijens FPT. 2003. Remodelling of continuously distributed collagen fibres in soft connective tissues. J Biomech. 36:1151–1158.

Driessen NJB, Wilson W, Bouten CVC, Baaijens FPT. 2004. A computational model for collagen fibre remodelling in the arterial wall. J Theor Biol. 226:53–64.

Ehlers W, Markert B, Röhrle O. 2009. Computational continuum biomechanics with application to swelling media and growth phenomena. GAMM Mitt. 32(2):135–156.

Ehret AE, Itskov M. 2007. A polyconvex hyperelastic model for fibre reinforced materials in application to soft tissues. J Mater Sci. 42:8853–8863.

Fisher GM, Llaurado JG. 1966. Collagen and elastin content in canine arteries selected from functionally different vascular beds. Circ Res. 19:394–399.

Garikipati K. 2009. The kinematics of biological growth. Appl Mech Rev. 62(3):030801.

Garikipati K, Arruda EM, Grosh K, Narayanan H, Calve S. 2004. A continuum treatment of growth in biological tissue: the coupling of mass transport and mechanics. J Mech Phys Solids. 52(7):1595–1625.

Gleason RL, Humphrey JD. 2004. A 2-d model of flow-induced alterations in the geometry, structure, and properties of carotid arteries. J Biomech Eng. 126:371–381.

Göktepe S, Abilez OJ, Parker KK, Kuhl E. 2010. A multiscale model for eccentric and concentric cardiac growth through sarcomerogenesis. J Theor Biol. 265:433–442.

Grytz R, Meschke G. 2010. A computational remodeling approach to predict the physiological architecture of the collagen fibril network in corneo-scleral shells. Biomech Model Mechanobiol. DOI 10.1007/s10237-009-0173-2.

Grytz R, Meschke G, Jonas JB. 2010. The collagen fibril architecture in the lamina cribrosa and peripapillary sclera predicted by a computational remodeling approach. Biomech Model Mechanobiol. DOI 10.1007/s10237-010-0240-8.

Hartmann S, Neff P. 2003. Polyconvexity of generalized polynomial-type hyperelastic strain energy functions for near-incompressibility. Int J Solids Struct. 40:2767–2791.

Himpel G. 2007. Computational modelling of biomechanical phenomena – remodelling, growth and reorientation. [PhD thesis]. [Germany]: Technical University Kaiserslautern.

Himpel G, Kuhl E, Menzel A, Steinmann P. 2005. Computational modelling of isotropic multiplicative growth. CMES. 8(2):119–134.

Himpel G, Menzel A, Kuhl E, Steinmann P. 2007. Time-dependent fibre reorientation of transversely isotropic continua – finite element formulation and consistent linearization. Int J Numer Methods Eng, DOI: 10.1002/nme.2124.

Holzapfel GA. 2000. Nonlinear solid mechanics. Chichester: Wiley.

Holzapfel GA. 2006. Determination of material models for arterial walls from uniaxial extension tests and histological structure. J Elasticity. 238:290–302.

Holzapfel GA, Gasser TC, Ogden RW. 2000. A new constitutive framework for arterial wall mechanics and a comparative study for material models. J Theor Biol. 61:1–48.

Hu J-J, Fossum TW, Miller MW, Xu H, Liu J-C, Humphrey JD. 2007. Biomechanics of the porcine basilar artery in hypertension. Ann Biomed Eng. 35(1):19–29.

Huiskes R, Weinans H, Grootenboer HJ, Delstra M, Fudala B, Slooff TJ. 1987. Adaptive-bone remodelling theory applied to prosthetic design analysis. J Biomech. 20:1135–1150.

Humphrey JD. 2001. Stress, strain, and mechanotransduction in cells. J Biomech Eng. 123:638–641.

Humphrey JD. 2002. Cardiovascular solid mechanics – cells, tissues, and organs. New York: Springer.

Humphrey JD, Rajagopal KR. 2002. A constrained mixture model for growth and remodeling of soft tissues. Math Models Methods Appl Sci. 12(3):407–430.

Itskov M, Ehret AE, Mavrilas D. 2006. A polyconvex strain–energy function for soft collagenous tissue. Biomech Model Mechanobiol. 5:17–26.

Kim YS, Galis ZS, Rachev A, Han H-C, Vito RP. 2009. Matrix metalloproteinase-2 and -9 are associated with high stresses predicted using a nonlinear heterogeneous model of arteries. J Biomech Eng. 131:1–10.

Klisch SM, Chen SS, Sah RL, Hoger A. 2003. A growth mixture theory for cartilage with application to growth-related experiments on cartilage explants. J Biomech Eng. 125: 169–179.

Klisch SM, van Dyke TJ, Hoger A. 2001. A theory of volumetric growth for compressible elastic biological materials. Math Mech Solids. 6:551–575.

Kondo S, Hashoimoto N, Kikuchi H, Hazama F, Nagata I, Kataoka H. 1997. Cerebral aneurysms arising at nonbranching sites. An experimental study. Stroke. 28:398–404.

Kuhl E, Holzapfel GA. 2007. A continuum model for remodeling in living structures. J Mater Sci. 42:8811–8823.

Kuhl E, Maas R, Himpel G, Menzel A. 2006. A continuum model for remodeling in living structures. J Mater Sci. 6(5): 321–331.

Kuhl E, Menzel A, Steinmann P. 2003. Computational modeling of growth – a critical review, a classification of concepts and two new consistent approaches. Comput Mech. 32:71–88.

Lee EH. 1969. Elastic–plastic deformations at finite strains. J Appl Mech. 36:1–6.

Machyshyn IM, Bovendeerd PHM, van de Ven AAF, Rongen PMJ, van de Vosse FN. 2010. A model for arterial adaptation combining microstructural collagen remodeling and 3D tissue growth. Biomech Model Mechanobiol, DOI 10.1007/s10237-010-0204-z.

Menzel A. 2005. Modelling of anisotropic growth in biological tissues. Biomech Model Mechanobiol. 3(3):147–171.

Menzel A. 2007. A fibre reorientation model for orthotropic multiplicative growth configurational driving stresses, kinematics-based reorientation, and algorithmic aspects. Biomech Model Mechanobiol. 6:303–320.

Menzel A, Waffenschmidt T. 2009. A microsphere-based remodelling formulation for anisotropic biological tissues. Philos Trans R Soc A. 367:3499–3523.

Nash MP, Hunter PJ. 2000. Computational mechanics of the heart. J Elasticity. 61:113–141.

Oden JT. 1972. Finite elements of nonlinear continua – an introduction. Vol. 1. New York: McGraw-Hill.

Ogden RW. 1997. Non-linear elastic deformations. Dover: Wiley.

Peng SH, Chang WV. 1997. A compressible approach in finite element analysis of rubber–elastic materials. Comput Struct. 62(3):573–593.

Pope A, Sands GB, Smaill B, LeGrice IJ. 2008. Three-dimensional transmural organization of perimysial collagen in the heart. Am J Heart Physiol. 295:H1243–H1252.

Richter G, Kellner A. 1963. Hypertrophy in the human heart at the level of fine structure. J Biomech. 18:195–206.

Rizzo RJ, McCarthy WJ, Dixit SN. 1989. Collagen types and matrix protein content in human abdominal aortic aneurysms. J Vasc Surg. 10:365–373.

Rodriguez EK, Hoger A, McCulloch AD. 1994. Stress-dependent finite growth in soft elastic tissues. J Biomech. 27:455–467.

Sanders JE, Goldstein BS. 2001. Collagen fibril diameters increase and fibril densities decrease in skin subjected to repetitive compressive and shear stresses. J Biomech. 34: 1581–1587.

Sands GB, Gerneke DA, Hooks DA, Green CR, Smaill BH, LeGrice IJ. 2005. Automated imaging of extended tissue volumes using confocal microscopy. Microsc Res Technol. 67:227–239.

Schmid H, Watton PN, Maurer MM, Winkler P, Wimmer J, Wang Y, Röhrle O, Itskov M. 2010. Impact of transmural heterogeneities on arterial adaptation – application to aneurysm formation. Biomech Model Mechanobiol. 9(3):295–315.

Spencer AJM. 1984. Constitutive theory for strongly anisotropic solids. In: Spencer AJM, editor. Continuum theory of the mechanics of fibre-reinforced composites. New York: Springer-Verlag.

Sturgis JE, Robinson JP, Voytik-Harbin SL. 2002. Tensile mechanical properties of three-dimensional type i collagen extracellular matrices with varied microstructure. J Biomech Eng. 124(2):214–223.

Taber LA. 1995. Biomechanics of growth, remodeling, and morphogenesis. Appl Mech Rev. 48(8):487–646.

Taber LA. 2001. Biomechanics of cardiovascular development. Annu Rev Biomed Eng. 3:1–25.

Taber LA. 2008. Theoretical study of Beloussov's hyper-restoration hypothesis for mechanical regulation of morphogenesis. Biomech Model Mechanobiol. 7:427–441.

Takamizawa K, Hayashi K. 1987. Strain energy density function and uniform strain hypothesis for arterial mechanics. J Biomech Eng. 20:7–17.

Takamizawa K, Hayashi K. 1988. Uniform strain hypothesis and thin-walled theory in arterial mechanics. Biorheology. 25:555–565.

Taylor RE, Zheng C, Jackson PR, Doll JC, Chen JC, Holzbaur KRS, Besier T, Kuhl E. 2009. The phenomenon of twisted growth: humeral torsion in dominant arms of high performance tennis players. Comput Methods Biomech Biomed Engin. 12:83–93.

Watton PN, Hill NA, Heil M. 2004. A mathematical model for the growth of the abdominal aortic aneurysm. Biomech Model Mechanobiol. 3:98–113.

Watton PN, Ventikos Y, Holzapfel GA. 2009. Modelling the growth and stabilization of cerebral aneurysms. Math Med Biol. 26(2):133–164.

Weiss J, Maker B, Govindjee S. 1996. Finite-element implementation of incompressible, transversely isotropic hyperelasticity. Comput Methods Appl Mech Engin. 135: 107–128.

Wolff J. 1892. Das Gesetz der transformation der knochen. Berlin: Hirschwald.

6. Appendix

This section depicts the derivation of the general analytical solution for incompressible uniaxial tension of a unit cube with varying volume growth for one constituent ($C = 1$) and for general isotropic growth. The material is assumed to be of isotropic Neo–Hookean response. The deformation is described by

$$\mathbf{F} = \mathbf{F}_e \mathbf{F}_g. \tag{25}$$

The elastic deformation gradient $\mathbf{F}_e$ and its related Cauchy–Green deformation tensor and Green–Lagrange strain tensor read as follows:

$$\begin{aligned}
\mathbf{F}_e &= \begin{pmatrix} \lambda_e & 0 & 0 \\ 0 & \lambda_e^{-1/2} & 0 \\ 0 & 0 & \lambda_e^{-1/2} \end{pmatrix}, \\
\mathbf{C}_e = \mathbf{F}_e^{\mathrm{T}}\mathbf{F}_e &= \begin{pmatrix} \lambda_e^2 & 0 & 0 \\ 0 & \lambda_e^{-1} & 0 \\ 0 & 0 & \lambda_e^{-1} \end{pmatrix}, \\
\mathbf{E}_e &= \frac{1}{2}(\mathbf{C}_e - \mathbf{I}),
\end{aligned} \tag{26}$$

whereas the growth deformation tensor $\mathbf{F}_g$ and its related Cauchy–Green deformation tensor and Green–Lagrange strain tensor read as follows:

$$\begin{aligned}
\mathbf{F}_g &= \begin{pmatrix} \lambda_g & 0 & 0 \\ 0 & \lambda_g & 0 \\ 0 & 0 & \lambda_g \end{pmatrix}, \\
\mathbf{C} &= \mathbf{F}_g^{\mathrm{T}}\mathbf{C}_e\mathbf{F}_g = \lambda_g^2\mathbf{C}_e, \\
\mathbf{E} &= \frac{1}{2}(\mathbf{C} - \mathbf{I}).
\end{aligned} \tag{27}$$

The determinants can then be expressed in the following form:

$$\begin{aligned}
&\det(\mathbf{F}_e) = 1, \quad \det(\mathbf{F}_g) = J_g = \lambda_g^3 = J = \det(\mathbf{F}), \quad \det(\mathbf{C}_e) = 1, \\
&\det(\mathbf{C}) = J_g^2 = \lambda_g^6.
\end{aligned} \tag{28}$$

Accordingly, the free energy Ψ and the second Piola–Kirchhoff stress tensor $\mathbf{S}$ (cf. Equation (24)) read as follows:

$$\begin{aligned}
\Psi &= \frac{1}{2}k\theta(\mathrm{tr}(\mathbf{C}_e) - 3) = k\theta\mathrm{tr}(\mathbf{E}_e), \\
\mathbf{S} &= 2\nu^{-2/3}\frac{\partial\Psi}{\partial\mathbf{C}_e} - p\mathbf{C}^{-1} = \nu^{-2/3}\frac{\partial\Psi}{\partial\mathbf{E}_e} - p\mathbf{C}^{-1} \\
&= k\theta\nu^{-2/3}\mathbf{I} - p\mathbf{C}^{-1},
\end{aligned} \tag{29}$$

where p is the hydrostatic pressure which is a consequence of the incompressibility constraint and $\theta = f/\nu = f/J_g$ the changing normalised density from Equation (21).

With this, the Cauchy stress tensor $\boldsymbol{\sigma}$ in the current configuration can be expressed as follows:

$$\boldsymbol{\sigma} = \mathbf{F}_e\mathbf{S}\mathbf{F}_e^{\mathrm{T}} = k\theta\nu^{-2/3}\mathbf{B}_e - p\mathbf{I} = k\theta\nu^{-2/3}\mathbf{B}_e - \hat{p}\mathbf{I}, \tag{30}$$

with $\mathbf{B}_e = \mathbf{F}_e\mathbf{F}_e^{\mathrm{T}}$ being the left elastic Cauchy–Green deformation tensor which has the same matrix components as $\mathbf{C}_e$ in the case of uniaxial extension or tension, yet with spatial-based vectors, i.e. living in the current configuration.

Remembering that $\nu = J_g = \lambda_g^3$, the hydrostatic pressure can be determined by the condition for stress-free faces in the y- and z-directions ($\sigma_{yy} = \sigma_{zz} = 0$):

$$\sigma_{yy} = \sigma_{zz} = k\theta\lambda_g^{-2}\lambda_e^{-1} - \hat{p} = 0 \quad \Rightarrow \quad \hat{p} = k\theta\lambda_g^{-2}\lambda_e^{-1}, \tag{31}$$

and thus finally,

$$\boldsymbol{\sigma} = k\theta\nu^{-2/3}(\mathbf{B}_e - \lambda_e^{-1}\mathbf{I}) = k\theta\lambda_g^{-2}(\mathbf{B}_e - \lambda_e^{-1}\mathbf{I}). \tag{32}$$

The force in the direction of stretch $F_x = \sigma_{xx}A_x$ with $A_x = \lambda_g^2\lambda_e^{-1}A_{\mathrm{ref}}$, where A_{ref} is the unit reference area with dimensions cm^2 is

$$\begin{aligned}
F_x &= \left\{k\theta\nu^{-2/3}\left(\lambda_e^2 - \lambda_e^{-1}\right)\right\} \cdot \left\{\lambda_g^2\lambda_e^{-1}\right\} \\
&= \left\{k\theta\lambda_g^{-2}\left(\lambda_e^2 - \lambda_e^{-1}\right)\right\} \cdot \left\{\lambda_g^2\lambda_e^{-1}\right\} = k\theta\left(\lambda_e - \lambda_e^{-2}\right) \\
&= k\frac{f}{\nu}\left(\lambda_e - \lambda_e^{-2}\right).
\end{aligned} \tag{33}$$

If one now wants to solve the equation for λ_e, it can be rearranged as follows:

$$\begin{aligned}
(k\theta)\lambda_e^3 - (F_x)\lambda_e^2 - k\theta = 0 \Leftrightarrow \\
a\lambda_e^3 + b\lambda_e^2 + c\lambda_e + d = 0,
\end{aligned} \tag{34}$$

which can be solved with Cardano's formula `http://mathworld.wolfram.com/cardanosformula.html`. Finally, with this at hand, one can use the solution to validate any numerical result from the FE code.